



# Proton induced thick target $\gamma$ -ray yields of light nuclei at the energy region $E_p = 1.0\text{--}4.1$ MeV

A. Savidou <sup>a</sup>, X. Aslanoglou <sup>b,\*</sup>, T. Paradellis <sup>c</sup>, M. Pilakouta <sup>c</sup>

<sup>a</sup> Institute of Nuclear Technology, Radiation Protection, NCSR "Demokritos", Aghia Paraskevi, Attiki, GR-153 10, Greece

<sup>b</sup> Department of Physics, The University of Ioannina, Ioannina, GR-451 10, Greece

<sup>c</sup> Institute of Nuclear Physics, NCSR "Demokritos", Aghia Paraskevi, Attiki, GR-153 10, Greece

Received 9 July 1998; received in revised form 17 November 1998

---

## Abstract

Excitation function measurements of thick target  $\gamma$ -ray yields were taken for the elements Li, B, F, Na, Mg, Al, Si and P after bombardment with protons at the energy interval  $E_p = 1.0\text{--}4.1$  MeV. The yields of all  $\gamma$ -rays emitted at  $E_p = 1.77$  and 4.0 MeV are tabulated and discussed. © 1999 Elsevier Science B.V. All rights reserved.

---

## 1. Introduction

Analytical techniques based on detection of X-rays or  $\gamma$ -rays have been widely used in the past for quantitative analysis of both bulk and trace elements. In particular, X-ray Fluorescence (XRF) and Proton Induced X-ray Emission (PIXE) are routinely used for the determination of heavy elements ( $Z > 17$ ). However, K and L lines corresponding to elements with  $Z < 17$  have low energy, suffer large absorption and therefore have very low detection efficiency. The detection of  $\gamma$ -rays following the deexcitation of residual nuclei after bombardment with low energy protons can be used as an alternative method in this mass region.

The nuclear reactions used are of the type (p,  $\gamma$ ), (p,  $p'\gamma$ ), (p, n $\gamma$ ) and (p,  $\alpha\gamma$ ). When these reactions are performed on light nuclei, the Coulomb barrier is low and the beam energy needed is usually low, so that it can be reached by small accelerators.

Proton Induced Gamma-ray Emission (PIGE) has been used in the past for the determination of light elements in a variety of materials [1–9]. Also, spectroscopic information concerning all the  $\gamma$ -rays emitted by light nuclei are available at certain energies, after the works of Anttila et al. [10] and Kiss et al. [11] at energies below 4.0 MeV and at an angle of detection  $\theta = 55^\circ$ . Although a large amount of information on  $\gamma$ -rays of light nuclei exists and PIGE has been used for the determination of certain elements [3–6,8,9], a method for simultaneous determination of many light nuclei is still lacking. The problems that have to be faced in that direction concern the overlap between

---

\* Corresponding author. Tel.: +30-651-47235; fax: +30-651-45631; e-mail: xaslanog@cc.uoi.gr

different reaction channels (nuclear reactions on different elements leading to the same residual nucleus and the same emitted  $\gamma$ -ray), selection of the  $\gamma$ -rays to be monitored so that maximum yield is obtained and correct application of the energy loss corrections [12,13].

In the present work we investigated the  $\gamma$ -rays emitted by the elements Li, B, F, Na, Mg, Al, Si and P at bombarding energies  $E_p = 1.77$  and 4.0 MeV at angle  $\Theta = 90^\circ$ . This angle was selected in order to avoid widening of the peaks due to Doppler effect. The energy  $E_p = 4.0$  MeV was selected as working energy, while the  $E_p = 1.77$  MeV was selected because it can be reached by small accelerators and the  $\gamma$ -ray yields are still measurable. The aim of this work was to select certain  $\gamma$ -rays from each element to be used in quantitative simultaneous analysis of the elements mentioned above. For an accurate determination of the composition of a sample, corrections have to be made based on stopping powers and cross sections, as Ishi suggested in Refs. [12,13]. For this reason, detailed excitation functions were taken at the energy range  $E_p = 1.0$ –4.1 MeV. The problem of overlapping between  $\gamma$ -rays of the elements under investigation and  $\gamma$ -rays from elements frequently used in industrial materials was also investigated.

## 2. Experimental procedure

The experiments were performed at the Institute of Nuclear Physics, NCSR “Demokritos”, Athens, Greece, using the 5.5 MV terminal voltage TANDEM TN11 accelerator of the laboratory. The proton beam was directed to the target via two sets of collimators of diameter 4 mm. The target was placed at an angle  $\Theta = 45^\circ$  with respect to the beam and was cooled at temperature  $10^\circ\text{C}$  using an ethyl alcohol refrigerator, in order to withstand high beam current. An electric potential of 300 V was applied on the target for electron suppression, to assure accurate measurement of the beam current.

The detector used was an intrinsic Germanium  $\gamma$ -ray detector, with a resolution of 1.9 keV at the  $E_\gamma = 1333$  keV  $\gamma$ -ray, placed at angle  $90^\circ$  with respect to the beam. The solid angle of the detector

was determined using an  $^{152}\text{Eu}$  source of known activity placed at the position of the target. The same source was also used for the determination of the efficiency of the detector.

The targets used were pellets of powder graphite and cellulose, mixed with less than 10% of a compound containing the element under investigation in the isotopic abundance found in nature. Four pellets of different concentration were prepared and analysed for each element.

Detailed spectra were taken for the elements Li, B, F, Na, Mg, Al, Si and P at energies  $E_p = 1.77$  and 4.0 MeV. The accumulated charge for each spectrum varied so that the spectra were characterised by good statistics and the small peaks were well shaped. Excitation functions were taken at the energy range 1.0–1.82 MeV in steps of 10 keV and between 2.2 and 4.1 MeV in steps of 50 keV. Spectra of heavier elements frequently found in industrial alloys and geological samples were also taken at energies 1.77 and 4.0 MeV in order to investigate the problem of accidental overlap of  $\gamma$ -rays between light and heavy elements. Natural metallic targets of the elements Fe, Mn, Co, Cu, Pb, Sn, Ti and Sn were used, while for the elements Br, Cl, Zn, Mo, V, K, Ca, Cr, Ni and N we used pellets of cellulose and graphite containing the above elements in concentrations 30–40% by weight.

## 3. Experimental results and analysis

The  $\gamma$ -rays produced at energies  $E_p = 1.77$  and 4.0 MeV together with the corresponding yields and the possible overlap with other  $\gamma$ -rays are tabulated in Table 1. The blanks in this table indicate that these  $\gamma$ -rays were not seen in the spectra. The yields given are corrected for the efficiency of the detector and reduced to yield of monoatomic target via the relation

$$\frac{Y}{Y_{\text{pel}}} = \frac{100}{C} \cdot \frac{S_{\text{pel}}(E)}{S(E)}, \quad (1)$$

where  $Y$  and  $Y_{\text{pel}}$  are the  $\gamma$ -ray yields of the monoatomic target and the pellet, respectively,  $S$  and  $S_{\text{pel}}$  the corresponding stopping powers,  $C$  is

Table 1

Characteristic  $\gamma$ -rays and yields for several elements. The yields are in units (counts/ $\mu\text{C}$  sr)

$E_\gamma$ (keV)	Reaction	$E_p = 1.77$ MeV			$E_p = 4.0$ MeV		
		Yield	Overlap	Yield	Yield	Overlap	Yield
429	${}^7\text{Li}(p, n\gamma){}^7\text{Be}$				$2.6 \times 10^7$	${}^{10}\text{B}(p, \alpha\gamma){}^7\text{Be}$	$1.1 \times 10^7$
478	${}^7\text{Li}(p, p'\gamma){}^7\text{Li}$	$5.0 \times 10^6$	${}^{60}\text{Ni}(p, \gamma){}^{61}\text{Cu}$	60	$8.1 \times 10^7$	${}^{55}\text{Mn}(p, n\gamma){}^{55}\text{Fe}$	$1.2 \times 10^6$
						${}^{60}\text{Ni}(p, \gamma){}^{61}\text{Cu}$	$8.4 \times 10^3$
429	${}^{10}\text{B}(p, \alpha\gamma){}^7\text{Be}$	$2.0 \times 10^6$			$1.1 \times 10^7$	${}^7\text{Li}(p, n\gamma){}^7\text{Be}$	$2.6 \times 10^7$
718	${}^{10}\text{B}(p, p'\gamma){}^{10}\text{B}$	$1.2 \times 10^4$			$3.0 \times 10^6$		
2125	${}^{11}\text{B}(p, p'\gamma){}^{11}\text{B}$				$1.1 \times 10^7$	${}^{37}\text{Cl}(p, \alpha\gamma){}^{34}\text{S}$	$4.0 \times 10^5$
						${}^{34}\text{S}(p, p'\gamma){}^{34}\text{S}$	$3.4 \times 10^4$
197	${}^{19}\text{F}(p, p'\gamma){}^{19}\text{F}$	$2.0 \times 10^5$	${}^{59}\text{Co}(p, p'\gamma){}^{59}\text{Co}$	60	$4.3 \times 10^7$		
1236	${}^{19}\text{F}(p, p'\gamma){}^{19}\text{F}$				$6.8 \times 10^6$		
1349	${}^{19}\text{F}(p, p'\gamma){}^{19}\text{F}$				$9.7 \times 10^6$		
1357	${}^{19}\text{F}(p, p'\gamma){}^{19}\text{F}$				$1.7 \times 10^7$	${}^{48}\text{Ti}(p, \gamma){}^{49}\text{V}$	$3.0 \times 10^4$
1459	${}^{19}\text{F}(p, p'\gamma){}^{19}\text{F}$				$2.9 \times 10^6$		
6129	${}^{19}\text{F}(p, \alpha\gamma){}^{16}\text{O}$	$4.2 \times 10^6$			$5.0 \times 10^7$		
440	${}^{23}\text{Na}(p, p'\gamma){}^{23}\text{Na}$	$1.2 \times 10^6$			$3.9 \times 10^7$		
1369	${}^{23}\text{Na}(p, \gamma){}^{24}\text{Mg}$	$4.4 \times 10^3$	${}^{27}\text{Al}(p, \alpha\gamma){}^{24}\text{Mg}$	$6.7 \times 10^3$			
1634	${}^{23}\text{Na}(p, \alpha\gamma){}^{20}\text{Ne}$	$2.4 \times 10^5$			$2.6 \times 10^7$		
1636	${}^{23}\text{Na}(p, p'\gamma){}^{23}\text{Na}$						
1951	${}^{23}\text{Na}(p, p'\gamma){}^{23}\text{Na}$				$3.1 \times 10^5$		
2391	${}^{23}\text{Na}(p, p'\gamma){}^{23}\text{Na}$				$5.1 \times 10^5$		
390	${}^{25}\text{Mg}(p, p'\gamma){}^{25}\text{Mg}$	$2.8 \times 10^2$			$4.5 \times 10^5$		
417	${}^{25}\text{Mg}(p, \gamma){}^{26}\text{Al}$	$2.0 \times 10^2$					
452	${}^{24}\text{Mg}(p, \gamma){}^{25}\text{Al}$	$2.8 \times 10^2$					
585	${}^{25}\text{Mg}(p, p'\gamma){}^{25}\text{Mg}$	$7.1 \times 10^3$			$1.2 \times 10^6$		
844	${}^{26}\text{Mg}(p, \gamma){}^{27}\text{Al}$	$2.7 \times 10^2$	${}^{27}\text{Al}(p, p'\gamma){}^{27}\text{Al}$	$1.5 \times 10^4$			
			${}^{55}\text{Mn}(p, \gamma){}^{56}\text{Fe}$	$2.0 \times 10^3$			
975	${}^{25}\text{Mg}(p, p'\gamma){}^{25}\text{Mg}$	$2.0 \times 10^2$			$4.7 \times 10^5$		
990	${}^{25}\text{Mg}(p, p'\gamma){}^{25}\text{Mg}$				$9.3 \times 10^4$	${}^{63}\text{Cu}(p, \gamma){}^{64}\text{Zn}$	$1.6 \times 10^5$
						${}^{64}\text{Zn}(p, p'\gamma){}^{64}\text{Mn}$	$1.9 \times 10^5$
1014	${}^{26}\text{Mg}(p, \gamma){}^{27}\text{Al}$	$3.7 \times 10^2$	${}^{27}\text{Al}(p, p'\gamma){}^{27}\text{Al}$	$4.8 \times 10^3$			
1369	${}^{24}\text{Mg}(p, p'\gamma){}^{24}\text{Mg}$				$6.5 \times 10^6$	${}^{27}\text{Al}(p, \alpha\gamma){}^{24}\text{Mg}$	$4.0 \times 10^6$
						${}^{55}\text{Mn}(p, n\gamma){}^{55}\text{Fe}$	$4.5 \times 10^5$
1380	${}^{25}\text{Mg}(p, p'\gamma){}^{25}\text{Mg}$				$1.1 \times 10^5$		
1612	${}^{25}\text{Mg}(p, p'\gamma){}^{25}\text{Mg}$				$1.0 \times 10^6$	${}^{37}\text{Cl}(p, n\gamma){}^{37}\text{Ar}$	$4.0 \times 10^5$
1809	${}^{26}\text{Mg}(p, p'\gamma){}^{26}\text{Mg}$				$9.7 \times 10^5$		
1965	${}^{25}\text{Mg}(p, p'\gamma){}^{25}\text{Mg}$				$7.1 \times 10^4$		
844	${}^{27}\text{Al}(p, p'\gamma){}^{27}\text{Al}$	$1.5 \times 10^4$	${}^{26}\text{Mg}(p, \gamma){}^{27}\text{Al}$	$2.7 \times 10^2$	$7.5 \times 10^6$	${}^{56}\text{Fe}(p, p'\gamma){}^{56}\text{Fe}$	$1.7 \times 10^6$
			${}^{55}\text{Mn}(p, \gamma){}^{56}\text{Fe}$	$2.0 \times 10^3$		${}^{59}\text{Co}(p, \alpha\gamma){}^{56}\text{Fe}$	$1.6 \times 10^5$
1014	${}^{27}\text{Al}(p, p'\gamma){}^{27}\text{Al}$	$4.8 \times 10^3$	${}^{26}\text{Mg}(p, \gamma){}^{27}\text{Al}$		$1.6 \times 10^7$		
1369	${}^{27}\text{Al}(p, \alpha\gamma){}^{24}\text{Mg}$	$6.7 \times 10^3$	${}^{23}\text{Na}(p, \gamma){}^{24}\text{Mg}$	$4.4 \times 10^3$	$4.0 \times 10^6$	${}^{24}\text{Mg}(p, p'\gamma){}^{24}\text{Mg}$	$6.5 \times 10^6$
						${}^{55}\text{Mn}(p, n\gamma){}^{55}\text{Fe}$	$4.5 \times 10^5$
1720	${}^{27}\text{Al}(p, p'\gamma){}^{27}\text{Al}$				$1.8 \times 10^5$		
1779	${}^{27}\text{Al}(p, \gamma){}^{28}\text{Si}$	$6.3 \times 10^3$					
2211	${}^{27}\text{Al}(p, p'\gamma){}^{27}\text{Al}$				$2.1 \times 10^6$		
2734	${}^{27}\text{Al}(p, p'\gamma){}^{27}\text{Al}$				$5.2 \times 10^4$		
2839	${}^{27}\text{Al}(p, \gamma){}^{28}\text{Si}$	$5.3 \times 10^2$					

Table 1 (Continued)

$E_\gamma$ (keV)	Reaction	$E_p = 1.77$ MeV			$E_p = 4.0$ MeV		
		Yield	Overlap	Yield	Yield	Overlap	Yield
755	$^{29}\text{Si}(p, p'\gamma)^{29}\text{Si}$				$2.5 \times 10^5$		
1266	$^{30}\text{Si}(p, \gamma)^{31}\text{P}$				$3.6 \times 10^5$	$^{31}\text{P}(p, p'\gamma)^{31}\text{P}$	$8.9 \times 10^6$
1273	$^{29}\text{Si}(p, p'\gamma)^{29}\text{Si}$				$8.7 \times 10^5$		
1779	$^{28}\text{Si}(p, p'\gamma)^{28}\text{Si}$				$1.0 \times 10^7$	$^{31}\text{P}(p, \alpha\gamma)^{28}\text{Si}$	$1.1 \times 10^6$
2028	$^{29}\text{Si}(p, p'\gamma)^{29}\text{Si}$				$8.8 \times 10^4$		
2233	$^{30}\text{Si}(p, \gamma)^{31}\text{P}$				$7.9 \times 10^4$	$^{31}\text{P}(p, p'\gamma)^{31}\text{P}$	$1.0 \times 10^5$
2235	$^{30}\text{Si}(p, p'\gamma)^{30}\text{Si}$					$^{31}\text{P}(p, \gamma)^{32}\text{S}$	
1266	$^{31}\text{P}(p, p'\gamma)^{31}\text{P}$				$8.9 \times 10^6$	$^{30}\text{Si}(p, \gamma)^{31}\text{P}$	$3.6 \times 10^5$
1779	$^{31}\text{P}(p, \alpha\gamma)^{28}\text{Si}$				$1.1 \times 10^6$	$^{28}\text{Si}(p, p'\gamma)^{28}\text{Si}$	$1.0 \times 10^7$
2230	$^{31}\text{P}(p, \gamma)^{32}\text{S}$	$1.7 \times 10^3$			$1.0 \times 10^5$	$^{30}\text{Si}(p, \gamma)^{31}\text{P}$	$7.9 \times 10^4$
2233	$^{31}\text{P}(p, p'\gamma)^{31}\text{P}$					$^{30}\text{Si}(p, p'\gamma)^{30}\text{Si}$	

the weight percent concentration of the element in the target used, and  $E$  the bombarding energy at which the correction for the stopping power is performed.

Out of all the  $\gamma$ -rays emitted by these elements after different type of nuclear reactions, we propose one  $\gamma$ -ray per element to be followed and analysed at each energy. The  $\gamma$ -rays proposed for the energies 1.77 and 4.0 MeV are listed in Table 2. The criterion for the selection of these  $\gamma$ -rays was the high intensity, low background underneath the peak and absence of overlap with reaction channels from other light elements. A brief discussion of the  $\gamma$ -rays selected follows.

*Determination of Li:* The  $\gamma$ -ray  $E = 478$  keV from inelastic scattering of protons on  $^7\text{Li}$  is the only  $\gamma$ -ray present in the spectrum at  $E_p = 1.77$

MeV. At  $E_p = 4.0$  MeV, the  $\gamma$ -ray  $E_\gamma = 429$  keV from the reaction  $^7\text{Li}(p, n\gamma)^7\text{Be}$  is also emitted, but has less intensity than the  $E_\gamma = 478$  keV and overlaps with the reaction channel  $^{10}\text{B}(p, \alpha\gamma)^7\text{Be}$ .

*Determination of B:* The  $\gamma$ -ray  $E_\gamma = 429$  keV is recommended for the bombarding energy 1.77 MeV, while for the  $E_p = 4.0$  MeV we propose the ray  $E_\gamma = 718$  keV.

*Determination of F:* For the energy  $E_p = 1.77$  MeV, the  $E_\gamma = 6129$  keV from the reaction  $^{19}\text{F}(p, \alpha\gamma)^{16}\text{O}$  is recommended. At energy  $E_p = 4.0$  MeV though, the  $E_\gamma = 197$  keV  $\gamma$ -ray is preferred because of the greater detector efficiency of that energy.

*Determination of Na:* In both  $E_p = 1.77$  and 4.0 MeV we propose the  $\gamma$ -ray  $E_\gamma = 440$  keV from the reaction  $^{23}\text{Na}(p, p'\gamma)^{23}\text{Na}$ . This ray is the most

Table 2  
Characteristic  $\gamma$ -rays for each element

Element	$E_p = 1.77$ MeV		$E_p = 4.0$ MeV	
	$\gamma$ -Ray (keV)	Reaction	$\gamma$ -Ray (keV)	Reaction
Li	478	$^7\text{Li}(p, p'\gamma)^7\text{Li}$	478	$^7\text{Li}(p, p'\gamma)^7\text{Li}$
B	429	$^{10}\text{B}(p, \alpha\gamma)^7\text{Be}$	718	$^{10}\text{B}(p, p'\gamma)^{10}\text{B}$
F	6129	$^{19}\text{F}(p, \alpha\gamma)^{16}\text{O}$	197	$^{19}\text{F}(p, p'\gamma)^{19}\text{F}$
Na	440	$^{23}\text{Na}(p, p'\gamma)^{23}\text{Na}$	440	$^{23}\text{Na}(p, p'\gamma)^{23}\text{Na}$
Mg	585	$^{25}\text{Mg}(p, p'\gamma)^{25}\text{Mg}$	585	$^{25}\text{Mg}(p, p'\gamma)^{25}\text{Mg}$
Al	1779	$^{27}\text{Al}(p, \gamma)^{28}\text{Si}$	1014	$^{27}\text{Al}(p, p'\gamma)^{27}\text{Al}$
Si			1779	$^{28}\text{Si}(p, p'\gamma)^{28}\text{Si}$
P			1266	$^{31}\text{P}(p, p'\gamma)^{31}\text{P}$

intense in the spectra and does not overlap with any other reaction channel.

**Determination of Mg:** The  $\gamma$ -ray  $E_\gamma = 585$  keV from the reaction  $^{25}\text{Mg}(p, p'\gamma)^{25}\text{Mg}$  is the most intense in the spectrum at both bombarding energies and is thus recommended.

**Determination of Al:** At  $E_p = 1.77$  MeV we propose the  $\gamma$ -ray  $E_\gamma = 1779$  keV from the reaction  $^{27}\text{Al}(p, \gamma)^{28}\text{Si}$ . At the energy  $E_p = 4.0$  MeV, the  $\gamma$ -ray  $E_\gamma = 1014$  keV has high intensity, does not overlap with any other reaction channel and has low background and therefore can be used for the analysis of Al at this energy.

**Determination of Si:** Since the first excited state of  $^{28}\text{Si}$  is located at  $E_X = 1779$  keV, there is no inelastic channel opened at  $E_p = 1.77$  MeV and the other reaction channels have very low  $\gamma$ -ray yield. Silicon can be determined only at  $E_p = 4.0$  MeV via the  $\gamma$ -ray  $E_\gamma = 1779$  keV from the reaction  $^{28}\text{Si}(p, p'\gamma)^{28}\text{Si}$ . This  $\gamma$ -ray is also emitted from the reaction  $^{31}\text{P}(p, \alpha\gamma)^{28}\text{Si}$ .

**Determination of P:** At  $E_p = 1.77$  MeV the  $\gamma$ -rays from reactions on P have very low yield and were not seen in the spectra. At  $E_p = 4.0$  MeV, most  $\gamma$ -rays emitted by P overlap with the corresponding rays from reactions on Si. We chose the  $\gamma$ -ray  $E_\gamma = 1266$  keV which is the most intense line.

**Determination of Si and P:** At  $E_p = 4.0$  MeV the  $\gamma$ -rays  $E_\gamma = 1779$  and  $1266$  keV are produced by reactions on both  $^{28}\text{Si}$  and  $^{31}\text{P}$ , with yields indicated in Table 1. Since the yields on  $^{28}\text{Si}$  and on  $^{31}\text{P}$  are largely different, Si can be monitored by the  $\gamma$ -ray  $E_\gamma = 1779$  keV and P can be monitored by the  $\gamma$ -ray  $E_\gamma = 1266$  keV. In the case of simultaneous determination of Si and P, the values of the yields can be used for the separation of the contributions of each element as:

$$C_{\text{Si}}R_{1,\text{Si}} + C_{\text{P}}R_{1,\text{P}} = K_1,$$

$$C_{\text{Si}}R_{2,\text{Si}} + C_{\text{P}}R_{2,\text{P}} = K_2,$$

where  $C_{\text{Si}}$  and  $C_{\text{P}}$  are the weight percent of Si and P, respectively,  $R_{i,\text{Si}}$ ,  $R_{i,\text{P}}$  the yield of  $\gamma$ -ray  $i$  due to the presence of 1% Si or P in the sample, and  $K_i$  the yield of  $\gamma$ -ray  $i$  in the spectrum.

The excitation functions for the  $\gamma$ -rays listed at Table 2 are shown in Figs. 1–4. For the  $\gamma$ -rays used

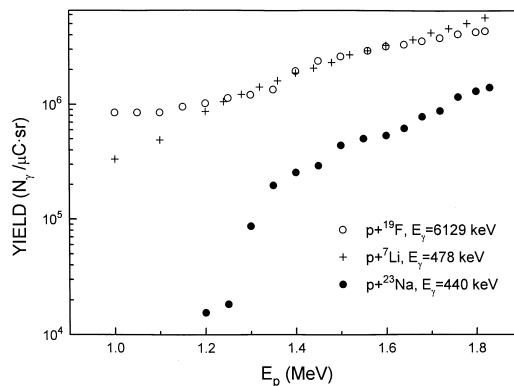


Fig. 1. Excitation functions for the elements F, Li and Na at the energy range 1.0–1.82 MeV.

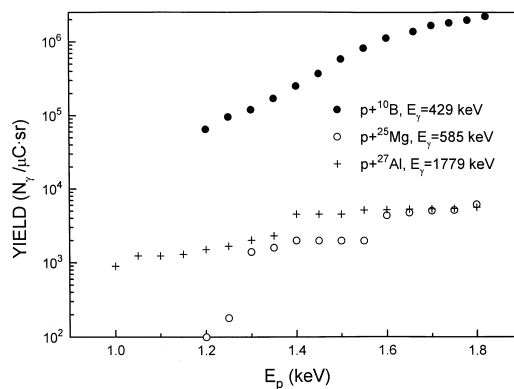


Fig. 2. Excitation functions for the elements B, Mg and Al at the energy range 1.0–1.82 MeV.

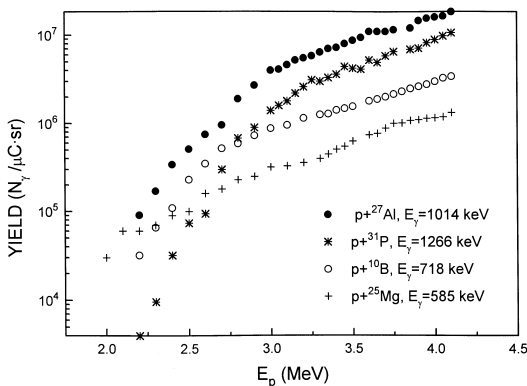


Fig. 3. Excitation functions for the elements Al, P, B and Mg at the energy range 2.2–4.1 MeV.

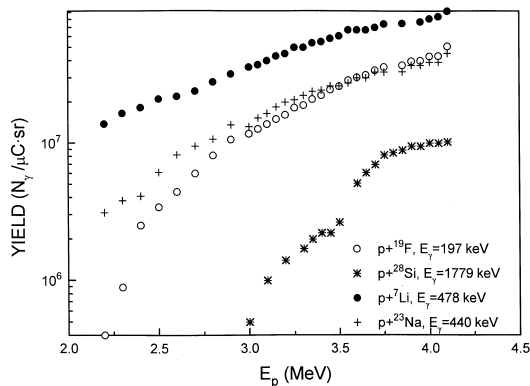


Fig. 4. Excitation functions for the elements F, Si, Li and Na at the energy range 2.2–4.1 MeV.

at energy  $E_p = 1.77$  MeV, the excitation functions were taken at the energy interval  $E_p = 1.0$ – $1.82$  MeV while for those  $\gamma$ -rays used at  $E_p = 4.0$  MeV the corresponding interval was  $E_p = 2.2$ – $4.1$  MeV. The data for the 585 keV  $\gamma$ -ray of  $^{25}\text{Mg}$  and the 1779 keV in Fig. 2 were taken from Refs. [4,2], respectively.

In a quantitative analysis for the determination of a certain element, usually a reference material (standard) of known concentration is measured and the concentration of the actual sample is deduced by an expression similar to Eq. (1), namely

$$\frac{Y_{\text{samp}}}{Y_{\text{ref}}} = \frac{C_{\text{samp}}}{C_{\text{ref}}} \cdot \frac{S_{\text{ref}}(E)}{S_{\text{samp}}(E)}, \quad (2)$$

where  $Y$ ,  $C$  and  $S$  are the yield, concentration and stopping power of the sample and the reference material, respectively. The stopping power corrections are performed at the mean energy  $E_m^{\text{act}}$  defined for thick target [13] as

$$E_m^{\text{act}} = \int_0^{E_0} \frac{\sigma(E)}{S(E)} / \int_0^{E_0} \frac{1}{E} \cdot \frac{\sigma(E)}{S(E)}$$

or

$$E_m^{\text{act}} = E_0 / \left( 1 + \frac{E_0}{Y_0(E_0)} \int_0^{E_0} \frac{Y_0(E)}{E^2} dE \right)$$

with

$$Y_0(E) = L \cdot \int_0^E \frac{\sigma(E)}{S(E)} dE \quad \text{and}$$

$$L = \frac{N \cdot F_A \cdot N_0 \cdot C}{A}.$$

In this expression  $E_0$  is the bombarding energy,  $\sigma(E)$  the reaction cross section,  $Y_0$  the thick target yield,  $N$  the Avogadro number,  $F_A$  the abundance percent of the isotope, and  $N_0$  and  $A$  are the number of beam ions on the target and the mass number of the element, respectively. An other point at which energy loss corrections are usually made is the energy  $E_{1/2}$ , at which the yield drops to one half of the initial one. The energy  $E_m^{\text{act}}$  depends on the composition of the sample, while  $E_{1/2}$  does not. Still, this dependence is small. In expression (2), the stopping powers were calculated at energy  $E_m^{\text{act}}$ . The energies  $E_{1/2}$  and  $E_m^{\text{act}}$  calculated for the graphite pellets using the excitation functions from the present work, are tabulated in Table 3. The stopping powers were calculated using the coefficients by Ziegler et al. [14].

#### 4. Applications

The method introduced above was applied in the analysis of a clay sample (Smectite Swy-1). The measurements were performed at both energies for the determination of F, Na, Mg, Al and Si, using the reference materials described in the present work. The specimens were dried at  $300^\circ\text{C}$  for 4 h before being used as targets. The remaining water was bound and was not affected by the beam. For

Table 3

The energies  $E_m^{\text{act}}$  and  $E_{1/2}$  obtained for the analysis of light elements using the shown  $\gamma$ -rays at  $E_p = 4.0$  MeV

Element	$E_\gamma$ (keV)	$E_m^{\text{act}}$ (MeV)	$E_{1/2}$ (MeV)
Li	478	2.79	3.10
B	718	3.25	3.46
F	197	3.22	3.36
Ma	440	3.00	3.22
Mg	585	3.22	3.48
Al	1014	3.31	3.43
Si	1779	3.53	3.60
P	1266	3.40	3.51

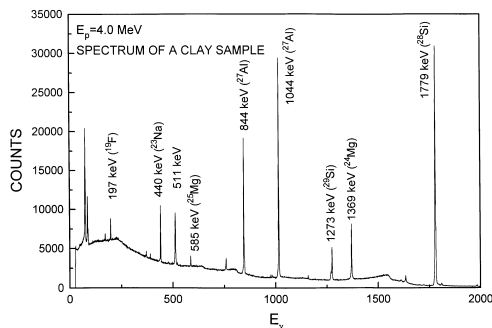


Fig. 5. Experimental spectrum of a clay at  $E_p = 4.0$  MeV.

Table 4  
Analysis of Smectite clay standard employing the present method (% by weight)

Element	PIGE at 4.0 MeV	PIGE at 1.77 MeV	Certified value
F	$0.11 \pm 0.01$	$0.12 \pm 0.01$	0.11
Na	$1.15 \pm 0.02$	$1.20 \pm 0.03$	1.13
Mg	$2.10 \pm 0.22$	$1.90 \pm 0.30$	1.86
Al	$10.20 \pm 0.10$	$9.80 \pm 0.03$	10.4
Si	$29.41 \pm 0.03$	–	29.3

the calculation of the stopping powers, a recursion process was followed. In the beginning the composition was assumed 20%  $\text{Al}_2\text{O}_3$ , 70%  $\text{SiO}_2$  and 10%  $\text{H}_2\text{O}$ . The stopping powers were evaluated using this composition and a newer more accurate composition was established. A new stopping power was then calculated based on that composition, etc. The process ends when the results do not change at the level of 1%.

The energy spectrum at  $E_p = 4.0$  MeV is shown in Fig. 5. The results of the analysis at both energies together with the certified composition of the material are presented in Table 4.

## 5. Discussion and conclusions

In the present work we investigated the yields of  $\gamma$ -rays emitted after nuclear reactions on light

elements such as Li, B, F, Mg, Na, Al, Si and P at proton energies 1.77 and 4.0 MeV. For each element and each energy, we selected one  $\gamma$ -ray line which combines high intensity and non-interference with other reaction channels, to be used in simultaneous quantitative analysis by PIGE. The intensity of the  $\gamma$ -rays observed was much higher at 4.0 MeV, but the lower energy (1.77 MeV) allows accurate analysis using small accelerators.

For the proper application of stopping power corrections, detailed excitation functions were taken at the energy range  $E_p = 1.0$ –4.1 MeV. Application of this technique for the analysis of a clay sample revealed results consistent with the certified values.

## References

- [1] G. Deconninck, J. Radioanal. Chem. 12 (1972) 157.
- [2] G. Deconninck, G. Demortier, J. Radioanal. Chem. 12 (1972) 189.
- [3] J.F. Chemin, J. Roturiet, B. Saboy, G.Y. Petit, J. Radioanal. Chem. 12 (1972) 221.
- [4] G. Demortier, P. Delsate, Radiochem. Radioanal. Lett. 21 (1975) 219.
- [5] A.L. Hanson, K.W. Jones, D.R. Corbin, Nucl. Instr. and Meth. B 9 (1985) 301.
- [6] G. Demortier, F. Bodart, J. Radioanal. Chem. 12 (1972) 209.
- [7] G. Deconninck, G. Debras, Radiochem. Radioanal. Lett. 20 (1975) 175.
- [8] H. Salah, B. Touchrift, Nucl. Instr. and Meth. B 129 (1997) 261.
- [9] M.J. Kenny, J.R. Bird, E. Clayton, Nucl. Instr. and Meth. 168 (1980) 115.
- [10] A. Anttila, R. Hanninen, J. Raisanen, J. Radioanal. Chem. 62 (1981) 293.
- [11] A.Z. Kiss, E. Koltay, B. Nyako, I.S. Somorial, A. Anttila, J. Raisanen, J. Radioanal. and Nucl. Chem. 89 (1985) 123.
- [12] K. Ishi, M. Valladon, J.L. Debrun, Nucl. Instr. and Meth. 150 (1978) 213.
- [13] K. Ishi, M. Valladon, C.S. Sastri, J.L. Debrun, Nucl. Instr. and Meth. 153 (1978) 503.
- [14] J.F. Ziegler, J.P. Biersack, U. Littmark, The Stopping and Range of Ions in Matter, vol. 1, Pergamon Press, New York, 1980.